

Primary Photophysics of Nicotinamide Chromophores in Their Oxidized and Reduced Forms

Mariana M. Reza, Jesús Durán-Hernández, Beatriz González-Cano, Jesús Jara-Cortés, Rafael López-Arteaga, Andrea Cadena-Caicedo, Leonardo Muñoz-Rugeles, Jesús Hernández-Trujillo, and Jorge Peon*



Cite This: *J. Phys. Chem. B* 2023, 127, 8432–8445



Read Online

ACCESS |



Metrics & More

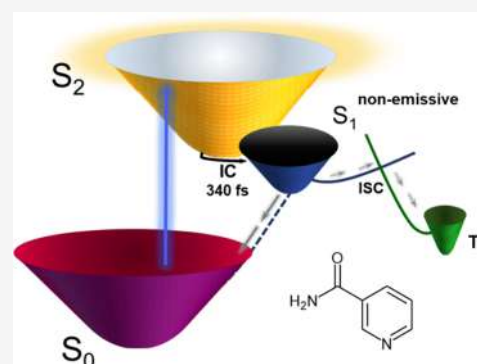


Article Recommendations



Supporting Information

ABSTRACT: Nicotinamide adenine dinucleotide (NADH) is an important enzyme cofactor with emissive properties that allow it to be used in fluorescence microscopies to study cell metabolism. Its oxidized form NAD^+ , on the other hand, is considered to produce negligible fluorescence. In this contribution, we describe the photophysics of the isolated nicotinamidic system in both its reduced and oxidized states. This was achieved through the study of model molecules that do not carry the adenine nucleotide since its absorbance would overlap with the absorption spectrum of the nicotinamidic chromophores. We studied three model molecules: nicotinamide (niacinamide, an oxidized form without nitrogen substitution), the oxidized chromophore 1-benzyl-3-carbamoyl-pyridinium bromide (NBzOx), and its reduced form 1-benzyl-1,4-dihydronicotinamide (NBz). For a full understanding of the dynamics, we performed both femtosecond-resolved emission and transient absorption experiments. The oxidized systems, nicotinamide and NBzOx, have similar photophysics, where the originally excited bright state decays on an ultrafast timescale of less than 400 fs. The depopulation of this state is followed by excited-state positive absorption signals, which evolve in two timescales: the first one is from 1 to a few picoseconds and is followed by a second decaying component of 480 ps for nicotinamide in methanol and of 80–90 ps for nicotinamide in methanol and NBzOx in aqueous solution. The long decay times are assigned as the S_1 lifetimes populated from the original higher-lying bright singlet, where this state is nonemissive but can be detected by transient absorption. While for NBzOx in aqueous solution and for nicotinamide in methanol, the S_1 signal decays to the solvent-only level, for the aqueous solutions of nicotinamide, a small transient absorption signal remains after the 480 ps decay. This residual signal was assigned to a small population of triplet states formed during the slower S_1 decay for nicotinamide in water. The experimental results were complemented by XMS-CASPT2 calculations, which reveal that in the oxidized forms, the rapid evolution of the initial $\pi-\pi^*$ state is due to a direct crossing with lower-energy dark $n-\pi^*$ singlet states. This coincides with the experimental observation of long-lived nonemissive states (80 to 480 ps depending on the system). On the other hand, the reduced model compound NBz has a long-lived emissive $\pi-\pi^*$ S_1 state, which decays with a 510 ps time constant, similarly to the parent compound NADH. This is consistent with the XMS-CASPT2 calculations, which show that for the reduced chromophore, the dark states lie at higher energies than the bright $\pi-\pi^*$ S_1 state.



INTRODUCTION

Reduced nicotinamide adenine dinucleotide (NADH) has the function of transporting electrons to feed the reducing steps inside the cell. To accomplish this function, the coenzyme is in redox equilibrium with its oxidized form (NAD^+). Specifically, NAD^+ is reduced to NADH in different steps during glycolysis and the Krebs cycle. This way, the electrons or reducing equivalents are transported by NADH into the mitochondria by specific membrane proteins. Once in the inner mitochondrial space, NADH is reoxidized by membrane enzymes responsible for oxidative phosphorylation. In addition, this dinucleotide acts as a donor of adenosine diphosphate-ribose (ADP-ribose) in ADP-ribosylation steps or as a precursor of the second messenger for cyclic ADP-ribose. Finally, the

oxidized form also has roles as an extracellular agent in regulatory processes.¹

The reduced form, NADH, is widely used in live cell microscopies as an intrinsic fluorescent reporter of cell metabolism,^{2,3} where the nicotinamide chromophore's first excited singlet state has a variable lifetime depending on whether it is in the free or protein-bound forms.^{4,5} The

Received: May 16, 2023

Revised: August 18, 2023

Published: September 21, 2023

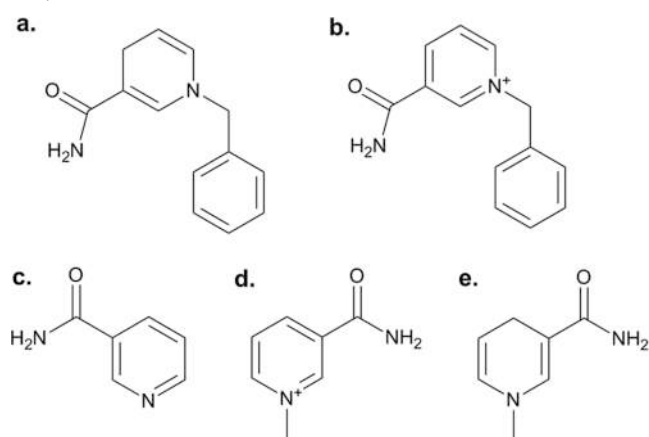


oxidized-state NAD^+ on the other hand is considered to be nonfluorescent. In order to have a better assessment of the intracellular metabolism, the relative emission signals of NADH and FAD (flavine adenine dinucleotide in its oxidized form) are used to determine cellular redox states, where NAD^+ and the reduced flavine (FADH_2) do not contribute to the fluorescence signals at any detection wavelength.^{6,7}

The emissive NADH molecule has a prominent absorption band at 260 nm where a significant fraction of the absorbance corresponds to adenine.^{8,9} This reduced form of the nicotinamide molecule has its lowest-energy band at 340 nm that corresponds to the first excited singlet, which is long-lived and significantly emissive.¹⁰ On the other hand, the oxidized form NAD^+ has a single absorption band in the ultraviolet (UV) region centered at 258 nm where the absorbance corresponds in part to the adenine moiety (83%) and in part to the oxidized nicotinamide ring (17%).¹¹

Due to the general interest in the mechanisms for the electronic deactivation of biologically important molecules^{12–14} and the relevance of these compounds in cellular sciences, we present here the first experimental and computational study of the intrinsic photophysics of the nicotinamide chromophore with a focus on the oxidized forms. For this, we explored three model systems: nicotinamide (niacinamide), 1-benzyl-1,4-dihydronicotinamide (NBz, a nicotinamide-only NADH model), and 1-benzyl-3-carbamoyl-pyridinium in the form of the bromide salt (NBzOx, a nicotinamide-only model for the oxidized form, NAD^+). The molecular structures are shown in Scheme 1. These model molecules are needed to

Scheme 1. Structures of the Molecules in this Study: (a) 1-Benzyl-1,4-dihydronicotinamide (NBz), (b) Its Oxidized Form 3-Carbamoyl-1-benzyl-pyridinium (NBzOx), (c) Nicotinamide, (d) 3-Carbamoyl-1-methyl-pyridinium (CMP), and (e) Its Reduced Form 1-Methyl-1,4-dihydronicotinamide (CMDHP)^a



^aThe first three molecules were studied by experimental means. The latter two molecules (d, e) are simplified systems used for the computational studies only.

study the nicotinamide excited states resulting from UV excitation without the interference of the adenine chromophore. A specific aim of this contribution is to characterize the excited-state dynamics of nicotinamidic systems to clarify the photophysical processes of the oxidized forms that relate to their negligible emissions.

The unsubstituted nicotinamide compound ((c) in Scheme 1) has several therapeutic usages, some of which are directly related to its photophysical properties. Specifically, it has been shown that this molecule has significant photoprotective effects when used topically on the skin or taken orally.^{15–17} In vivo studies on mice models have shown that photoinduced carcinogenesis and immunosuppression can be inhibited by the topical application of nicotinamide formulations. In those studies, the effects of topical nicotinamide were related to a reduction of UV-induced suppression of antigenic tumor rejection.¹⁸ In other studies, it has been shown that nicotinamide reduces UV-induced proliferation of melanocytes.¹⁹ These types of effects have been associated with a sunscreen-type effect by the nicotinamide molecule itself or by nicotinamide adducts formed with the components of different skin layers. The UV light absorption, excited-state evolution, and energy dissipation properties of this heterocycle, described herein, are related to these effects.

In the present study, the primary photoinduced channels of nicotinamidic systems were explored through fluorescence upconversion and transient absorption spectroscopies. As we show below, the combination of subpicosecond time resolution of the emission and transient absorption measurements is crucial to understand these systems since this allows the discrimination between bright and dark excited states. For a better understanding of the photophysics, the experiments were complemented by high-level excited-state quantum mechanical calculations of the model compounds under the perspective given by the potential energy surfaces of each system. The minimum energy path beginning in the Franck–Condon region provided mechanistic information to support the interpretation of the experimental results. In particular, the presence and accessibility of conical intersections in the initially populated bright states are central to understand the deactivation processes.^{20–22}

In the Results and Discussion section, we include a brief review of the photophysics of pyridine and related systems as explored previously by femtosecond spectroscopies in the gas and solution phase.^{23,24} This is followed by comparisons between the nicotinamidic systems and other biologically important heterocycles, which provides insights about the role of the carbamoyl substituent that give nicotinamidic systems their specific photophysics.

MATERIALS AND METHODS

Nicotinamide was obtained from Sigma-Aldrich, with a purity greater than 99.5%; NBz was purchased from TCI Chemicals, with a purity greater than 95%. The standard molecule, coumarin 102 (C102), was acquired from MP Biomedicals. Laser-grade *p*-terphenyl with high-performance liquid chromatography (HPLC) quality was purchased from Sigma-Aldrich. NBzOx was synthesized by a nucleophilic substitution reaction from nicotinamide based on the work of Paul.²⁵ A white powder was obtained with a melting point of 112–116 °C, and its structure was confirmed by magnetic resonance and mass spectroscopies. The systems were purified by a two-solvent recrystallization method employing methanol and acetone.

Steady-State Spectroscopy. The absorbance and fluorescence spectra were obtained in a quartz cell with a 1 cm optical path in a Cary-50 spectrophotometer and a Cary Eclipse fluorometer, respectively. To calculate the fluorescence yield of NBz, we used C102/methanol as the reference. On the other hand, *p*-terphenyl was used as the reference for NBzOx

and nicotinamide. For the yields, the standards were prepared in methanol, and the index of refraction was taken into consideration. All of the experiments were carried out in controlled temperature conditions (20 ± 1 °C).

Time-Resolved Fluorescence Measurements. The optical arrangement of the ultrafast time-resolved fluorescence technique is described in more detail in our group's publications.^{26–28} In brief, the system is based on a regenerative Ti/sapphire amplifier which produces laser pulses centered at 760 or 800 nm with a duration of 150 fs and a repetition rate frequency of 1 kHz. The beam was divided into three parts: the first was sent to a delay stage and served as the gate pulse in the fluorescence upconversion setup. The second beam was directed to another delay stage and reached a sum frequency mixing β -BBO crystal to generate the third harmonic of the fundamental pulses through a sum frequency mixing scheme with the second harmonic beam. Finally, the third branch was brought to another β -BBO crystal to obtain the second harmonic of the fundamental pulse (380 or 400 nm, depending on the fundamental wavelength). The resulting pulses were mixed with the second branch for the third harmonic generation. The third harmonic pulses were separated from the residual fundamental and the second harmonic with a two-prism compressor setup and were sent to a flow cuvette with a 30 cm focal length CaF_2 lens so that the beam waist was 0.1 mm at the sample. The polarization of the excitation beam was adjusted with a half waveplate to the magic angle (54.7°) with respect to the direction of the acceptance axis of a third β -BBO crystal where the fluorescence upconversion process was realized between the sample's fluorescence and the delayed gate pulses.

The sample was kept flowing continuously through a 1 mm quartz cell, and the fluorescence was collected and refocused with a pair of parabolic mirrors. The upconverted signal was focused to the input of a double 10 cm monochromator (Oriel); and was detected with a photomultiplier tube connected to a lock-in amplifier (Stanford Research Systems) referenced to a phase-locked optical chopper at one-third of the laser repetition rate. The instrument response function (IRF) for the upconversion experiments was determined from the methanol Raman signals or the rise of the emission signal on the red side of the spectrum of coumarin C102 in methanol. The IRF was Gaussian with an fwhm of 150 to 300 fs, depending on the detection wavelength.

Transient Absorption Measurements. The transient absorption setup used the same Ti/sapphire laser, centered at 800 nm, and the same third harmonic generation scheme to form 266 nm pulses. The continuum probe pulse was generated from the fundamental output by using a 2 mm sapphire plate. The pump and probe spot diameters at the sample were measured to be 0.85 and 0.1 mm, respectively, by a knife-edge scan at the sample position. The pump pulse was used to excite the sample, which was kept flowing continuously through a 1 mm path-length quartz cell. The pump pulse energy was kept at less than $0.5 \mu\text{J}$ in order to minimize the formation of solvated electrons through solvent ionization. The probe pulses were spectrally isolated with a double monochromator and detected with a silicon photodiode connected to a lock-in amplifier (SR830, Stanford Research Systems) referenced to a phase-locked optical chopper synchronized to 1/3 of the repetition rate of the laser.²⁹ The instrumental response function (IRF) for the transient absorption experiments was determined from fits to con-

volved biexponential traces of the well-known dye coumarin 153. The IRF was considered to be a Gaussian function. The 400 fs full width at half-maximum of this Gaussian was determined as a fitting parameter of the convoluted function.

Computational Section. The stationary points (equilibrium geometries and transition states), minimum energy conical intersections (MECIs), and intrinsic reaction coordinates were obtained with the XMS-CASPT2 multiconfigurational method using the cc-pVDZ basis set. In order to reduce the computational cost, simplified systems were studied instead of NBz and NBzOx, where the benzyl groups bonded to the heterocyclic nitrogens were replaced with a methyl group. The simplified molecules are shown in Scheme 1 and are 3-carbamoyl-1-methylpyridinium (CMP, a NBzOx proxy) and 1-methyl-1,4-dihydronicotinamide (CMDHP, a NBz proxy). The vertical electronic transition energies and oscillator strengths for the NBz and NBzOx molecules at their equilibrium geometries were also computed to make comparisons to the smaller model systems. Tables S2–S9 and Figures S7–S14 of the Supporting Information present the corresponding results for nicotinamide and the CMDHP-NBz and CMP-NBzOx pairs for comparison purposes. In both cases (for each pair), the low-energy excited electronic states are centered on the nicotinamide fragment and have the same character. This provides support for the use of CMP and CMDHP to rationalize the photophysical behavior of NBz and NBzOx. The cc-pVDZ basis set was used for computational efficiency because the Hessian matrix is calculated numerically, a prohibitive procedure for larger basis sets. Tables S7–S9 and Figure S15 of the Supporting Information present the dependence of the electronic energies in terms of the basis set size. They show that switching from double- to triple- ζ or including diffuse functions causes a slight decrease in the energies; however, the same mechanistic picture is obtained (see below). To avoid the intruder state problem, a level shift of 0.3 was used in all cases. The nature of the stationary points was verified by evaluating the vibrational frequencies. The active spaces of the CASSCF wave functions comprise m electrons in o orbitals (n , π , or π^* in nature) and are given by the (m , o) pairs as follows: (12,10) for (CMP), (12,9) for CMDHP, and (12,10) for nicotinamide. The electronic structure calculations were carried out with the BAGEL program.³⁰

RESULTS AND DISCUSSION

Steady-State Spectroscopy. The absorption, emission, and excitation spectra of NBz in methanol are shown in Figure 1. This solvent was used due to the limited solubility of NBz in water solution. The absorption spectrum has its first band at a maximum at 350 nm. The emission spectrum has a maximum at 450 nm. The fluorescence yield for this molecule was 0.05; this fluorescence efficiency is comparable with that of NADH.^{31,32}

NBzOx is an analogue chromophore to the oxidized nicotinamidic ring in NAD^+ but without the adenine heterocycle so that the dynamics upon direct excitation of this pyridinium type system can be studied without signal overlaps from the adenine nucleotide.⁸ In Figure 2, we show the absorption spectrum of NBzOx in water, which has a single band in this region but at a much shorter wavelength in comparison with the first band of NBz. The absorption maximum occurs at 266 nm and corresponds to a molar extinction coefficient of $4059 \text{ M}^{-1} \text{ cm}^{-1}$. The spectra of the

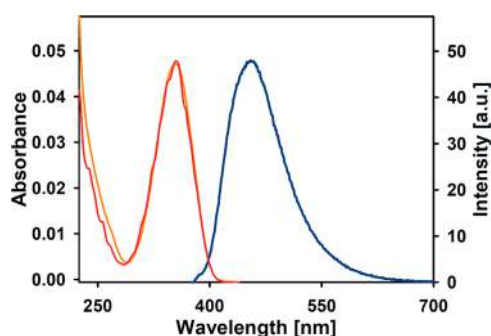


Figure 1. Absorption (left axis, orange), emission (right axis, blue; $\lambda_{\text{exc}} = 360$ nm), and excitation (right axis, red; $\lambda_{\text{emi}} = 500$ nm) spectra of 1-benzyl-1,4-dihydroxynicotinamide (NBz) in methanol.

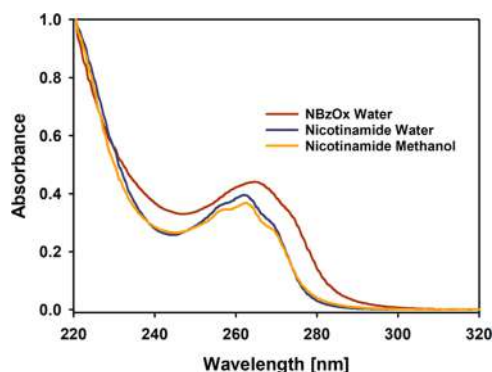


Figure 2. Absorption spectra of nicotinamide in water (blue) and methanol (yellow) and of 1-benzyl-3-carbamoyl-pyridinium bromide (NBzOx) in water (red).

nicotinamide system are also shown in Figure 2 (in methanol and water). In this case, the spectra have a maximum at 260 nm, and an extinction coefficient of $2670 \text{ M}^{-1} \text{ cm}^{-1}$.³³

Oxidized nicotinamides are considered “nonfluorescent”. Although we attempted to detect steady-state emissions from NBzOx and nicotinamide samples in HPLC-grade methanol or ultrapure water, these molecules produce negligible steady-state signals that cannot be distinguished from the solvent-only baselines. From this, the fluorescence quantum yields from NBzOx and nicotinamide can be established to be below a value of 1×10^{-5} using *p*-terphenyl as a standard for both molecules.³⁴

Femtosecond Fluorescence Upconversion Experiments. We studied the time evolution of the emissions from the NADH analogue (reduced form) NBz to characterize the intrinsic excited-state dynamics of the reduced heterocycle bonded to the carbamoyl chromophoric unit and to contrast these results with those of the oxidized nicotinamide system. In the NBz heterocycle (as in NADH), the carbon on the opposite side of the nitrogen heteroatom is bonded to two hydrogen atoms. With this, the chromophoric unit corresponds to a linear conjugation from one double bond on the opposite side of the carbamoyl moiety, continuing through the nitrogen heteroatom and then continuing with a second double bond, terminating at the carbonyl and amino groups. This is obviously a significant structural difference with respect to the aromatic oxidized pyridinium ring of NAD^+ .

The excitation wavelength for these measurements was 380 nm for direct excitation into the first band of NBz. The experiments were exclusively performed in methanol due to

the solubility of NBz, which is limited in water. The single-wavelength traces are included in Figure 3a and required two

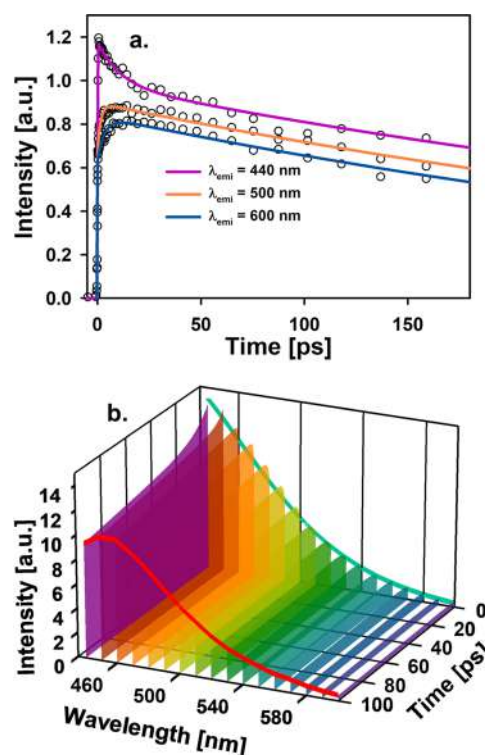


Figure 3. (a) Fluorescence upconversion transients of 1-benzyl-1,4-carbamoyl-pyridine (NBz) detected at different wavelengths in methanol. (b) Time-resolved emission spectra of NBz in methanol. NBz was excited at a wavelength of 380 nm.

exponential terms for an appropriate fit. The longer time constant was obtained by a global fit of the signals from 420 to 600 nm showing a fluorescent-state lifetime of 510 ps. The shorter time constant for these traces varies across the spectrum and corresponds to exponential decay terms of several picoseconds below 460 nm and rising terms above this wavelength. The effect of these picosecond features in the time-resolved emission spectra can be seen in Figure 3B, and show a dynamic Stokes shift as the spectrum’s maximum moves from 430 nm at $t = 0$ to 450 nm in equilibrium. The time constants related to this shift are around 7 ps (Table S1). From such timescale and considering that 380 nm corresponds to an excitation wavelength near the $S_1(0-0)$ vibronic transition, this picosecond shift is assigned to solvation in methanol.^{9,14,35,36} The sensitivity of this chromophore to the relaxation of its solvent shells means that it probably could be used as a probe for environment relaxation in proteins.^{37,38} We also performed experiments on NBz with 266 nm excitation to compare directly with the experiments on NBzOx and nicotinamide, where the first transitions correspond to a 266 nm-centered band. The respective traces for excitation at 266 nm are included in the Supporting Information for representative wavelengths (Figure S1). The only difference between the 266 and the 380 nm experiments for NBz is that the rising time constants at the red side of the emission spectra are slower by a factor of three to four in comparison with the 380 nm excitation experiments.

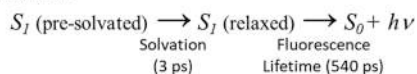
As can be seen in Figure 1, the 266 nm excitation produces higher excited singlet states since the S_1 band is well-defined

and has its high-energy edge at 300 nm. This excitation energy (266 nm) corresponds to approximately 1.5 eV above the S_1 state $v = 0$ level (0–0 transition at 400 nm, see Figure 1). This implies that the relaxation within the emissive state involves a significant amount of vibrational cooling after the rapid internal conversion to the emissive state ($S_n \rightarrow S_1$, typically sub-200 fs, not detected). Several studies have distinguished that vibrational relaxation into the lowest level of the emissive state is associated with band narrowing and shifting.³⁹ More specifically, it has been observed that diverse vibrational energy transfer steps involving methanol as solvent do take place in the timescale of 1 to 15 ps,⁴⁰ which is consistent with the time constants of the early evolution of the NBz emission spectrum after 266 nm excitation.

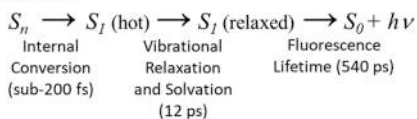
Independent of the excitation wavelength, the first excited singlet in the reduced chromophore is long-lived, with a lifetime of 510 ps. The fluorescence lifetime of NBz is similar to that of NADH in its unbound form of 447 ps.⁴¹ A summary of the photophysics of the reduced nicotinamidic chromophore considering both excitation wavelengths is included in Scheme 2. As we show next, the NBz signals differ drastically in comparison with the models for the oxidized form NAD^+ .

Scheme 2. Observed Photophysical Processes for the Reduced Nicotinamidic Chromophore (NBz)

380 nm excitation:



266 nm excitation:



The time-resolved emission results for nicotinamide and NBzOx are shown in the top graphs of Figures 4 to 6. The NBzOx molecule is a close analogue of the oxidized nicotinamidic ring in NAD^+ , including the quaternized form of the heterocyclic nitrogen bonded to an aliphatic carbon atom. The nicotinamide molecule is also an analogue of NAD^+ , but in this case, the pyridinic nitrogen is not quaternized. NBzOx was studied in aqueous solution, and nicotinamide was studied in water and in methanol where it has good solubility, to check for any solvent dependence. For these experiments, due to the single band in the UVC region, the excitation was set to 266 nm. The fluorescence upconversion transients for solutions of these molecules are extremely short-lived and significantly weak. For both molecules (including methanol for nicotinamide), the upconversion transients show a subpicosecond decay in the 340 to 370 nm region, returning to a level at or near the baseline with time constants below 400 fs. At a wavelength of 360 nm, the traces appear to not return fully to the baseline but remain at 1 to 3% of the level of the amplitude of the decaying component considering our signal-to-noise ratio. This behavior is shown in the insets of Figures 4a, 5a, and 6a. The time evolution of the remaining signal after the first picoseconds at these wavelengths could not be determined due to the extremely low signal level, the intrinsic small sensitivity of the upconversion experiments, and instrumental limitations.

The most important feature of the upconversion transients of the oxidized forms is the sharp difference with the case of

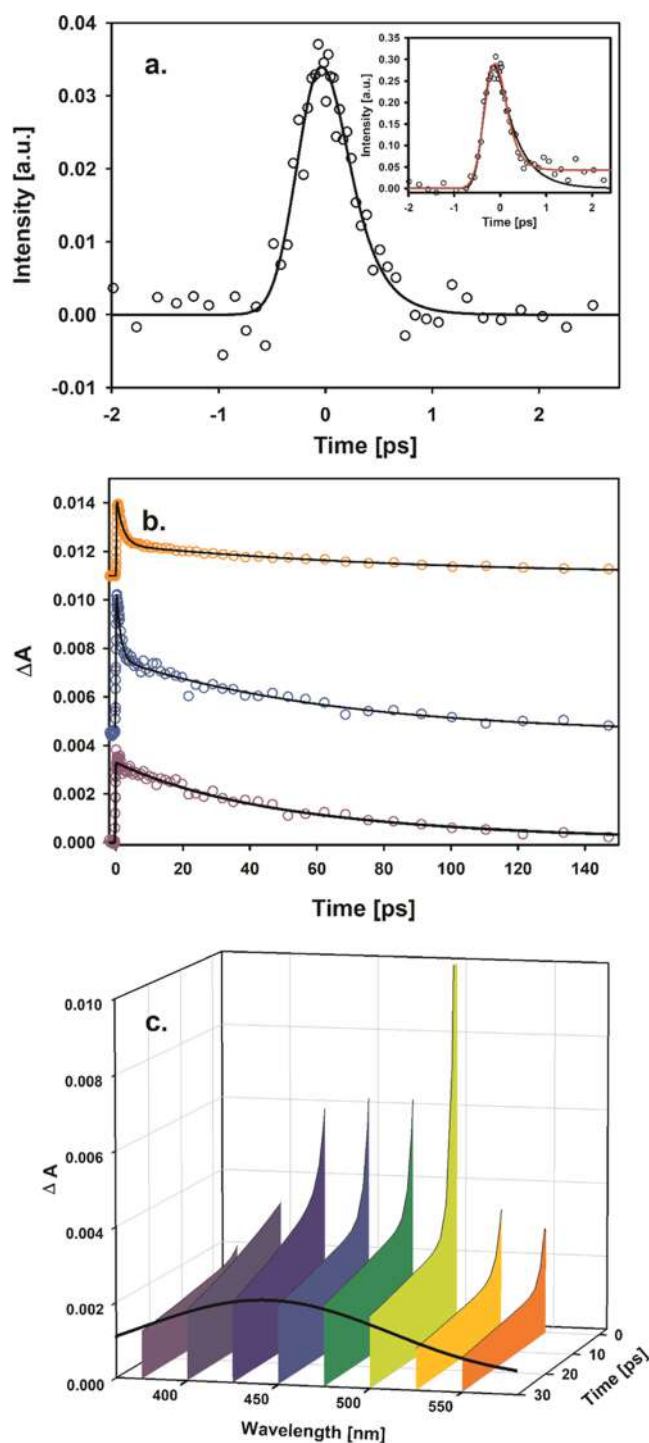


Figure 4. Time-resolved experiments for the oxidized form of 1-benzyl-1,4-carbamoyl-pyridine (NBzOx) in aqueous solution. The excitation wavelength in all cases was 266 nm. (a) Fluorescence upconversion experiments with detection at 340 nm (main plot) and 360 nm (inset). The inset shows a single exponential fit (black line) and a single exponential with a constant offset fit (red line) convoluted with the IRF. (b) Transient absorption traces at three representative wavelengths: 550 nm (orange), 475 nm (blue), and 400 nm (purple). (c) Transient absorption spectral profile obtained from the multiexponential fits of the single-wavelength traces. The transient absorption spectrum shown at 30 ps (black line) was acquired by scanning the transient signals with a monochromator and recording the signal every 12 nm.

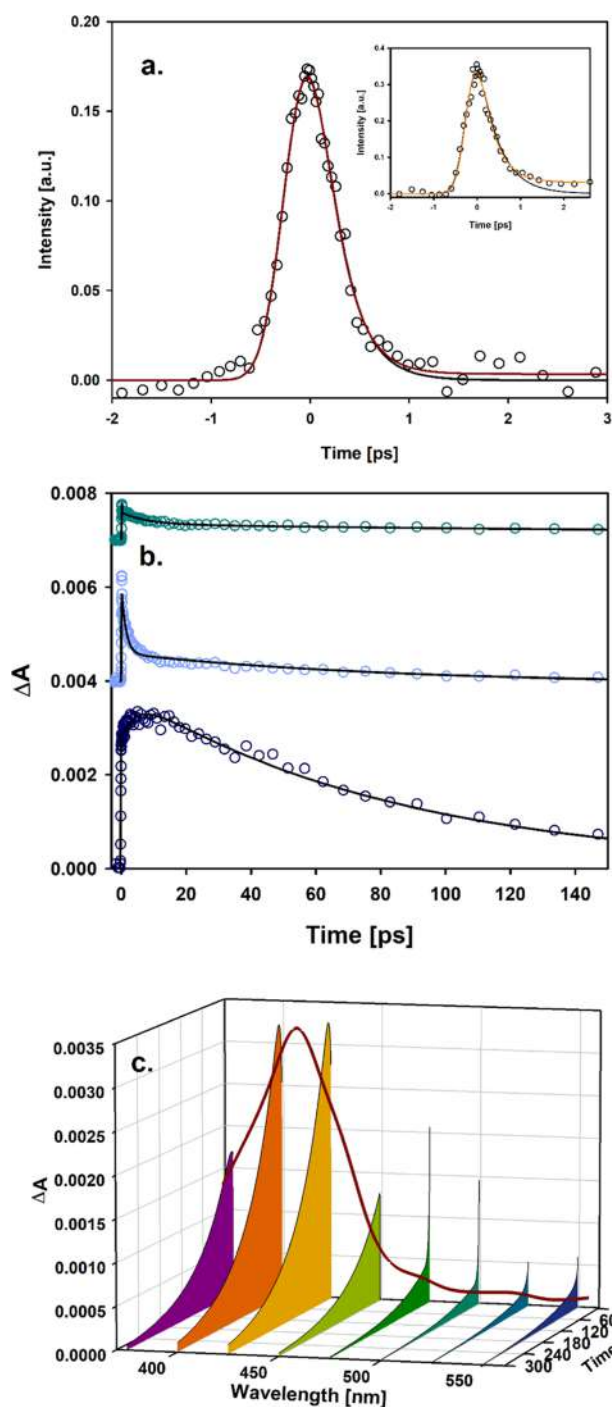


Figure 5. Time-resolved experiments for nicotinamide in a methanol solution. The excitation wavelength in all cases was 266 nm. (a) Fluorescence upconversion experiments with detection at 340 nm (main plot) and 360 nm (inset). The plots show a single exponential fit (black line) and exponential plus constant fit (dark red line or orange line for the inset) convoluted with the IRF. (b) Transient absorption traces at three representative wavelengths: 550 nm (teal), 475 nm (light blue), and 425 nm (dark blue). (c) Transient absorption spectral profile obtained from the multiexponential fits of the single-wavelength traces. The transient absorption spectrum shown at 30 ps (red line) was acquired by scanning the transient signals using a monochromator and recording the signal every 12 nm.

the reduced form NBz. We show a direct comparison of these traces in Figure S2. While the time-resolved emission traces for

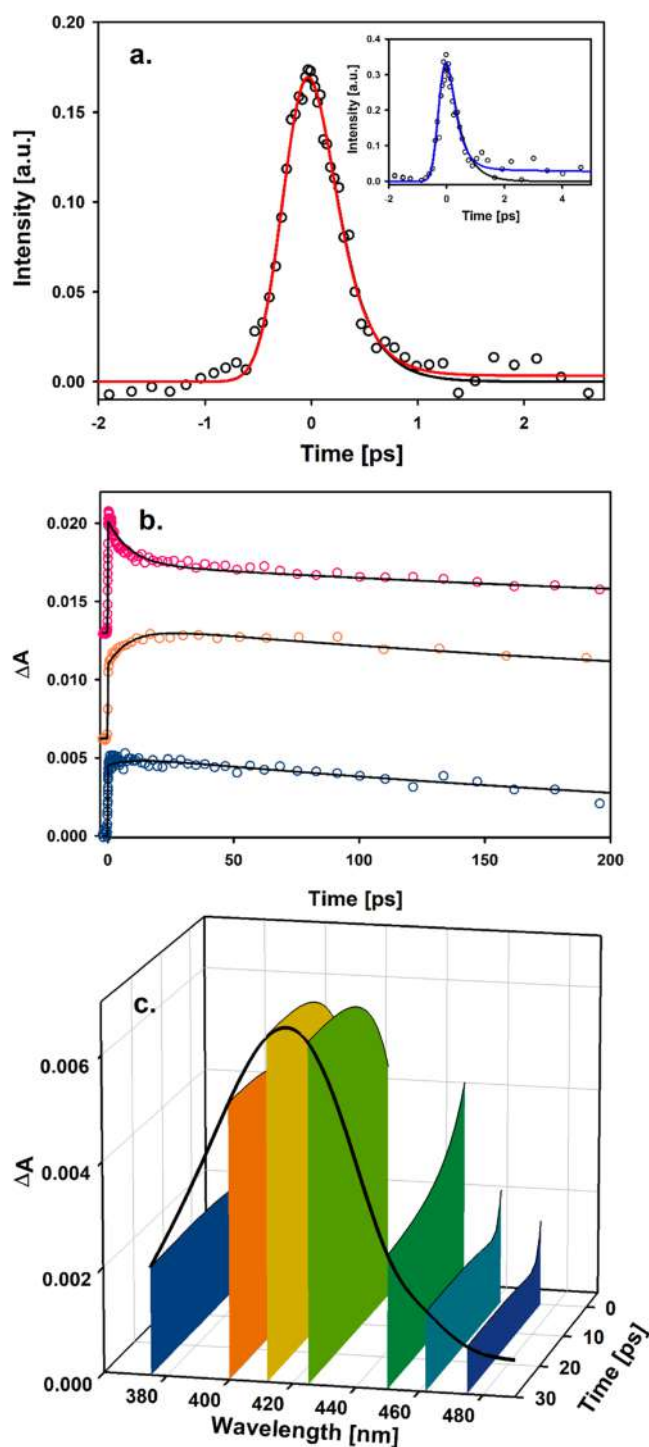


Figure 6. Time-resolved experiments for nicotinamide in an aqueous solution. The excitation wavelength in all cases was 266 nm. (a) Fluorescence upconversion experiments with detection at 340 nm (main plot) and 360 nm (inset). The plots shows a single exponential fit (black line) and exponential plus constant fits (red line or blue line for the inset) convoluted with the IRF. (b) Transient absorption traces at three representative wavelengths: 450 nm (pink), 405 nm (orange), and 375 nm (blue). (c) Transient absorption spectral profile obtained from the multiexponential fits of the single-wavelength traces. The transient absorption spectrum shown at 30 ps (black line) was acquired by scanning the transient signals using a monochromator and recording the signal every 12 nm.

NBz show that for the reduced form, there is a long-lived highly emissive singlet (which is responsible for the important quantum yield in the reduced nicotinamidic fluorophores and responsible for the NADH emission so commonly observed in biochemistry and cellular biology experiments), in the oxidized chromophores, the emission is nearly undetectable and only shows appreciable amplitude in the subpicosecond timescale.

From the timescales of the decays ($\tau < 400$ fs) and similarly to other systems,^{20,22} it can be interpreted that the originally accessed excited states of both NBzOx and nicotinamide upon excitation in the first band evolve on a potential energy surface that directly reaches a state crossing point. After this crossing, the resulting population corresponds to a dark or minimally emissive state or potentially to the ground state. Given the results from the **Computational Results** section (see below), which indicate the presence of other low-lying excited states below the first bright state, it was crucial to perform transient absorption studies to determine the possible evolution of the system from the bright initial state. It should be mentioned that no photochemical (dissociative or other) channels have been reported for NAD⁺.

Transient Absorption Measurements. Transient absorption measurements can reveal the presence of excited states (including singlets) which have a negligible oscillator strength for transitions to/from the electronic ground state but have signals associated with transitions to higher singlets.^{23,42,43}

We performed transient absorption measurements for NBzOx in aqueous solution and for nicotinamide in water and methanol solutions using an excitation wavelength of 266 nm. It is worth mentioning that excitation with 266 nm pulses in water and alcohol solutions commonly result in the production of solvated electrons due to multiphoton ionization of the solvent.^{44,45} The broad absorption feature from the solvated electrons frequently overlaps with the solute's transient $S_n \rightarrow S_m$ signals from single photon excitation. This issue implies a bit of a challenge for transient experiments since it is necessary to use—as low as possible—excitation intensities at the sample to minimize or eliminate the nonlinear solvent ionization events. In particular, the oxidized nicotinamidic systems have small oscillator strengths for transient absorption signals due the small size of this chromophore. From this, we needed to use intensities as low as 0.1 GW/cm², which enabled us to have negligible or the smallest possible solvent contributions in the transient signals. As can be seen in the traces in the Supporting Information (Figure S3), for nearly all of the transient absorption experiments, the contribution of the solvated electron was negligible as the amplitudes remain at the $t < 0$ level for the solvent-only experiments (taken back-to-back with the respective solution traces). Only for the case of nicotinamide/methanol at 450, 500, and 550 nm, there is an appreciable amount of signal in the solvent-only traces. These three solvent-only experiments show the typical behavior from photoionized electrons in methanol which are associated with the solvation and relaxation of the photoelectrons.⁴⁶ In agreement with previous observations, these background signals correspond to rising components to a constant level in this timescale.⁴⁷ The amplitude of this background signal was fitted to a simple exponential rise to a constant level and was subtracted from the experimental data only for the nicotinamide/methanol case at the three mentioned wavelengths. As we show in the **Supporting Information**, the amplitude of this solvent-only signal is very

small (of the order of 3%) and does not alter the evolution of the nicotinamide/methanol solution experiments (in fact, the respective time constants only change within the experimental uncertainty).

The transient absorption results for the NBzOx and nicotinamide solutions are included in **Figures 4** and **6**. At most wavelengths, the traces can be described with biexponential functions, although at certain wavelengths, a third component was required for adequate fits. The largest amplitudes in these traces are associated with long decay components with time constants of 82 ps for NBzOx in methanol and 84 ps for nicotinamide in methanol (see below for the nicotinamide/water case). These components are associated with the decays of broad transient absorption bands centered at 425 nm for both NBzOx/water and nicotinamide/methanol, as shown in **Figures 4c** and **5c**. The spectra shown at 30 ps for each trace were acquired in experiments where the signal was scanned across the spectrum. Within the signal-to-noise ratio in our experiments, the transients for NBzOx/water and nicotinamide/methanol decay to the baseline or solvent-only level after the 82 or 84 ps components. This is consistent with a minimal to negligible presence of long-lived transient species like photoproducts or triplet states, which we estimate that at most would account to a small percent of the signal amplitude for these two cases. In addition to the long 82 and 84 ps decays of the 425 nm-centered bands, the signals show early modulations on the timescale of 1 to a few picoseconds. These intermediate components could not be adjusted to a single value through global fitting. For the nicotinamide/methanol system, the intermediate components (up to a few ps) show positive amplitudes (decays) in the spectral region below the 425 nm maximum and negative components (rises) near the maxima and on the red side of this maximum. For both NBzOx/water and nicotinamide/methanol, the picosecond features produce a spectral blue shift and a clear narrowing of the 425 nm transient absorption bands within the first few picoseconds (see below). At some wavelengths, the early development of the transients actually shows subpicosecond rising components as we highlight in **Figure 7**, where the trace at 550 nm of NBzOx/water does not correspond to an instrument-limited rise but requires a negative-amplitude exponential component of 340 fs. To emphasize this, **Figure 7**

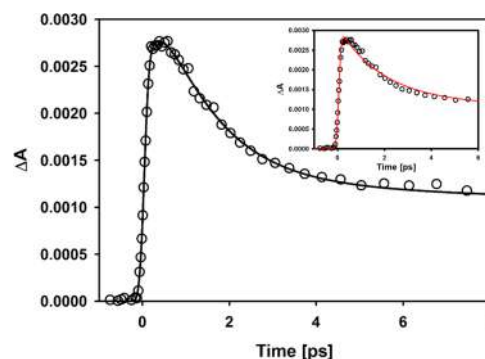


Figure 7. Transient absorption trace for NBzOx in aqueous solution 550 nm after excitation with a 266 nm subpicosecond pulse. The main graph includes a convoluted fit (black line) to a three-exponential function convoluted with the IRF, including a subpicosecond rise. For comparison, the inset shows the same trace with a double exponential convoluted fit without the early rising component, showing a systematic deviation between the data and the fit.

shows a comparison between the convoluted fits involving a rising component and an instrument-limited signal onset. We were able to characterize these rising components only in the region around 500 to 550 nm, verifying that this effect is not related to a $t \approx 0$ modulation frequently seen in these experiments (coherent “spike”). The parameter sets of the exponential fits for these systems are included in Tables 1–3.

Table 1. Global-Fitting Parameters for Selected Transient Absorption Traces of 1-Benzyl-3-carbamoyl-pyridinium Bromide (NBzOx) in Water^a

λ_{abs} [nm]	α_1	τ_1 [ps]	α_2	τ_2 [ps]
375	0.00027	1.5	0.0018	82
400	0.0013	1.0	0.0020	82
425	0.0018	1.9	0.0031	82
450	0.0034	1.5	0.0030	82
475	0.0033	1.4	0.0031	82
500 ^b	0.020	1.3	0.0028	82
525	0.0018	1.8	0.0016	82
550 ^b	0.0027	1.3	0.0013	82

^aThe long decay component of 388 ps was determined through global fitting. ^bIn addition to the biexponential components, a 340 fs rising component was detected at 500 and 550 nm.

Table 2. Global-Fitting Parameters for Selected Transient Absorption Traces of Nicotinamide in Methanol^a

λ_{abs} [nm]	α_1	τ_1 [ps]	α_2	τ_2 [ps]
375	-0.00029	7.0	0.0020	84
400	-0.0013	4.3	0.0038	84
425	-0.0011	4.5	0.0038	84
450	0.0015	4.5	0.0013	84
475	0.00099	3.0	0.00052	84
500	0.00059	3.0	0.00030	84
525	0.00016	7.2	0.00030	84
550	0.00023	7.3	0.00023	84

^aThe long decay component of 84 ps was determined through global fitting.

Table 3. Global-Fitting Parameters for Selected Transient Absorption Traces of Nicotinamide in Water^a

λ_{abs} [nm]	α_1	τ_1 [ps]	α_2	τ_2 [ps]	α_3	τ_3 [ps]
375			-0.00019	7.5	0.0022	480
400			-0.0022	7.5	0.0056	480
412			-0.0026	7.5	0.0070	480
425			-0.0024	7.5	0.0069	480
450			0.0016	7.5	0.0027	480
462	0.0011	1.2	-0.00037	7.5	0.0016	480
475	0.0010	1.2	-0.00027	7.5	0.00096	480

^aAt most wavelengths only two exponentials were required to fit the data (τ_2 , τ_3) while at 462 and 475 nm a third exponential was required.

As shown in Figure 6c, for the nicotinamide/water system, the transient signals are also dominated by the formation and decay of a broad transient absorption band at 425 nm; in this case, the long decay component is 480 ps. Similar to the previous cases, the onset of this band is accompanied by earlier components around 7.5 ps, which similarly show positive amplitudes on the red side of the 425 nm band and negative components near the band maximum and on the blue side of

the band, similar to the case of NBzOx and nicotinamide in methanol. At two wavelengths, 462 and 475 nm, a third, 1.2 ps exponential was required for an adequate fit.

For the nicotinamide/water system, the 480 ps decays do not return to the solvent-only levels but show a small component of persistent transient absorbance signals that do not show further evolution within at least 3 ns. The spectrum of this long-lived species was acquired in an independent experiment and is shown in Figures 8 and S4. As can be seen,

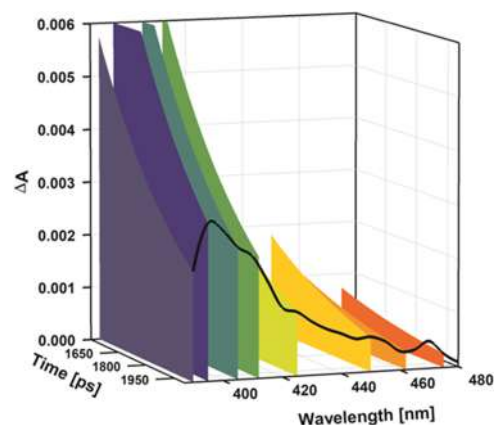


Figure 8. Transient spectrum for nicotinamide/water taken at a delay of 2 ns after a 266 nm excitation pulse.

this long-lived signal corresponds to a spectrum centered at 405 nm, which is different from the 425 nm band which develops in a subpicosecond timescale. From this, it is clear that the state responsible for the 425 nm band for nicotinamide in water partially evolves toward the formation of a long-lived state with a different spectrum and with a much smaller absorbance amplitude.

In summary, three oxidized systems, NBzOx/water, nicotinamide/methanol, and nicotinamide/water show a subpicosecond decay of the emission signals (upconversion traces), which is followed by the subpicosecond to picosecond relaxation into the state associated with the 425 nm band in all cases. The 425 nm bands in turn decay with time constants of 82, 84, and 480 ps, respectively, and then, only for nicotinamide/water, there is a persistent species associated with the 405 nm-centered band, which decays in timescales longer than a few nanoseconds.

Considering these results together, the subpicosecond decay of the originally excited bright state from the fluorescence upconversion experiments and the presence of subpicosecond features in some of the transient absorption traces are indicative of the initial formation and rapid decay (sub-400 fs) of the bright singlet state responsible for the UV ground-state absorption bands in the two oxidized nicotinamidic molecules. The formation of longer-lived transient absorption signals with a band at 425 nm for the three systems is consistent with the following photophysical pathway: The original bright state rapidly evolves into a different excited state with minimal-to-absent oscillator strength for radiative transitions to the ground state, given the long-lived 425 nm transient absorption band shown in Figures 4c, 5c, and 6c. Given slower decay of the 425 nm band, these long-lived signals can be readily assigned to the lowest-energy excited singlet of these heterocycles, where the 425 nm bands correspond to the main $S_1 \rightarrow S_n$ transition signal. As we

show in the next section, the computational results show the presence of $n-\pi^*$ nonemissive excited states which serve as gateways for the decay of the electronic excitation after the initial population of the bright $\pi-\pi^*$ states. The intermediate picosecond signal modulations (1 to several ps) lead to a small blue shift and bandwidth reduction of the 425 nm bands of Figures 4c, 5c, and 6c. The width of the 425 nm transient absorption band of nicotinamide in methanol and water (Figures 5 and 6) as a function of time is shown in Figure S5. As can be seen, this band undergoes a reduction in its full width at half-maximum with time constants of 3.5 and 8 ps (methanol and water, respectively). Several studies have observed that narrowing in the bandwidth of S_1-S_n bands are a sign of structural and vibrational relaxation within the S_1 state. It has been observed that the rate of the narrowing depends on several parameters, including the vibrational modes that contribute to the observed transitions.^{39,48} This implies that a variety of timescales can be observed for vibrational cooling. For methanol and water, several timescales have been observed, and the dynamics are typically multi-exponential involving similar time constants as those involved in the early evolution of the 425 nm band of nicotinamide.^{48–49,51} For the 425 nm band of the oxidized nicotinamidic systems, it is expected that initially the population of molecules in the S_1 state carries excess vibrational energy due to the formation of higher vibronic states from the initial $\pi-\pi^*$ to $n-\pi^*(S_1)$ population transfer (internal conversion, see also the Computational Results section).^{48,50,51} We then interpret the small picosecond amplitude evolutions associated with changes in the shape of the 425 nm band in the oxidized systems as signatures of relaxation steps within the S_1 state, influencing the shape of this S_1-S_n band observed through the pump–probe experiments.

For the case of nicotinamide/water and related to the longer-lifetime of the S_1 state, the decay of this state (S_1) is accompanied by a small yield for the formation of a long-lived state associated with the persistent 405 nm band, which is ascribed as the first triplet state of nicotinamide. Although to the best of our knowledge, this is the first time-resolved study on nicotinamide, and previous studies in low-temperature matrices have detected phosphorescence emissions from this molecule, which indicates that intersystem crossing can be an available channel for this system.^{52,53}

With relation to the rapid (subpicosecond) formation of the dark S_1 state from the original bright singlet, this kind of behavior has been observed for other nitrogen-heterocyclic systems, where the lowest excited singlet state has been referred to as a “trapped S_1 state” in the case of pyrimidinic DNA bases.^{12,42,54,55} The present results indicate that this is also the main photophysical pathway upon electronic excitation in the oxidized forms of nicotinamide. Clearly, the energy ordering of the dark and emissive singlet states in the oxidized vs reduced forms of this heterocycle changes drastically. Specifically, in the reduced form, the first excited singlet is highly emissive with a long lifetime of 510 ps. Further details about the nature of the excited singlet states involved in the photophysics of NBzOx and nicotinamide come from computational work.

Computational Results. To better understand the experimental results, we carried out a series of electronic structure calculations for the model compounds of NADH and NAD⁺. The compounds for these studies are models for the

experimentally studied systems as the phenyl groups in NBz and NBzOx were replaced by a methyl group to facilitate the calculations. Note that the benzyl groups in NBz and NBzOx are not involved at all in the photophysics of these molecules given the lack of extended conjugation. Comparisons between the results for the model systems and calculations on NBz or NBzOx are included in the Supporting Information. These calculations show the same state-ordering for vertical transitions between the model compounds (CMP and CMDHP) and the actual molecules (NBzOx and NBz, respectively; see Tables S2 to S6). The structures for the calculations are included in Scheme 1 and correspond to 3-carbamoyl-1-methylpyridinium (CMP), its reduced form, 1-methyl-1,4-dihydropyridinone (CMDHP), and nicotinamide. The minimum energy path (MEP) for the first bright excited state starting from the Franck–Condon region and the presence of energy barriers to access to the S_1/S_0 seam space were analyzed in the so-called static approach.^{56,57} Table 4

Table 4. Vertical Transition Energies (E_{abs} , eV) and Oscillator Strengths for the Lowest Singlet Electronic Transitions of 3-Carbamoyl-1-methylpyridinium (CMP), Nicotinamide, and 1-Methyl-1,4-dihydropyridinone (CMDHP)^a

transition	CMP			nicotinamide		
	type	E_{abs}	f	type	E_{abs}	f
$S_0 \rightarrow S_1$	$1^1n-\pi^*$	4.07	0.00	$1^1n-\pi^*$	4.58	0.001
$S_0 \rightarrow S_2$	$2^1n-\pi^*$	4.49	0.00	$1^1\pi-\pi^*$	4.86	0.008
$S_0 \rightarrow S_3$	$1^1\pi-\pi^*$	4.88	0.04	$2^1\pi-\pi^*$	4.90	0.004
	CMDHP					
	type	E_{abs}	f			
$S_0 \rightarrow S_1$	$1^1\pi-\pi^*$	3.83	0.18			
$S_0 \rightarrow S_2$	$1^1n-\pi^*$	4.75	0.00			
$S_0 \rightarrow S_3$	$2^1\pi-\pi^*$	5.81	0.00			

^aType refers to the orbital nature of the transition.

shows the vertical transition energies and oscillator strengths for the lowest-energy ground-state conformers of these molecules (Figure S6 shows front and side views of the S_0 equilibrium structures). Good agreement was observed between the experimental traces and the computational results. For example, the $S_0 \rightarrow S_1$ ($\pi-\pi^*$) transition for the fluorescent system CMDHP (NBz analogue) of 3.83 eV ($f = 0.18$) compares well with the 3.45 eV value observed for the first absorption band maximum of NBz in methanol. Also, the 4.86 eV ($S_0 \rightarrow S_2$) vertical transition to the first ($1^1\pi-\pi^*$) bright state calculated for nicotinamide compares well with the experimental value of 4.69 eV in methanol for this molecule. Similarly, the first calculated bright transition ($S_0 \rightarrow S_3$) for CMP lies at 4.88 eV, where the first observed band maximum in methanol for NBzOx is at 4.66 eV. Importantly, the calculations clearly reveal that for CMDHP, the lowest-energy excited state has significant oscillator strength ($1^1\pi-\pi^*$) but that for both CMP and nicotinamide, there is at least one dark state of $1^1n-\pi^*$ nature below the spectroscopically allowed states. For CMP, two $1^1n-\pi^*$ states (S_2 , S_1) exist at lower energies for the ground-state geometry, while a single $1^1n-\pi^*$ (S_1) state exists below the respective bright S_2 state of nicotinamide. In both molecules, the n-orbital associated with these transitions involves the carbamoyl substitution. The character of these states is described in the Supporting

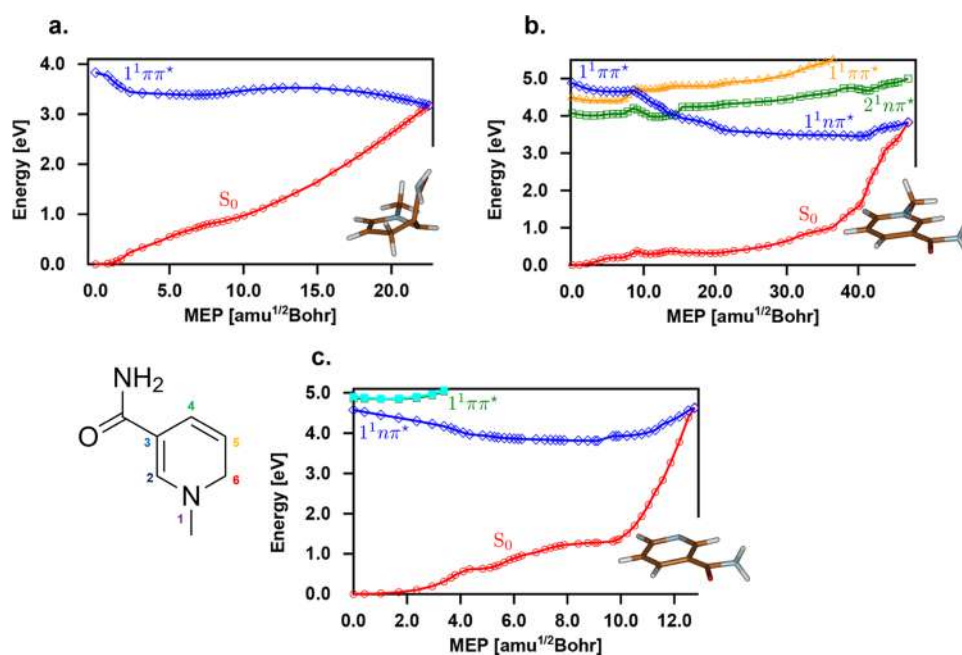


Figure 9. Energies of the lowest singlet electronic states along the $1^1\pi\pi^*$ minimum energy path of (a) reduced 1-methyl-4-carbamoyl-pyridine (CMDHP), (b) oxidized 3-carbamoyl-1-methylpyridinium (CMP), and (c) nicotinamide.

Information in Tables S2–S4, and accompanying Figures S7–S9. As we elaborate below and are in full agreement with the experimental results, these dark states are crucial in the photophysics of the oxidized nicotinamidic molecules.

A clear view of the photophysics of these molecules arises from the exploration of their potential energy surfaces and the evaluation of the different state crossings and relevant energy barriers. Figure 9 shows the energies of the lowest singlet electronic states along the $1^1\pi-\pi^*$ MEPs of the three molecules. In this figure, the most accessible profiles ending in the seam space are included. Several structures for minimal energy conical intersections (MECIs) were found (with lower singlet states). Their energetic relevance to the MEP was tested for CMP and CMDHP with an exploratory search using linear interpolation in internal coordinates starting from the vertically accessed geometries. The results of these searches are shown in Figures S10 and S11. From this analysis, only the most relevant pathways were included in our description.

For the case of CMDHP, as shown in Figure 9a, the main geometrical distortion toward the seam space with the electronic ground state is the C2=C3 bond twisting. This trajectory shows an energy barrier of 0.14 eV in the path toward the crossing of the S₁ and S₀ states. Moreover, the vertical S₁ → S₀ transition at the optimized geometry of the S₁ energy minimum is 2.67 eV (462.66 nm), which compares quite well with the band centered at 459.53 nm for the emission spectrum of NBz. This barrier along the MEP of CMDHP directly explains the fluorescence properties of NADH and NBz, including the 510 ps lifetime of its S₁($1^1\pi-\pi^*$) state.

The analysis is more interesting for the case of CMP which is shown in Figure 9b. In this case, there are dark states involved on the photophysical deactivation. First, the MEP proceeds on the state $1^1\pi-\pi^*$ until rapidly an S₃ minimum is reached. At this geometry, a rather small energy barrier of 0.03 eV gives access to an MECI in the S₃/S₂ seam space. After the crossing, a change in the nature of the electronic state from

$1^1\pi-\pi^*$ to $1^1n-\pi^*$ takes place, and the MEP proceeds through an S₂/S₁ crossing until it reaches the minimum geometry of the S₁ state (also of $1^1n-\pi^*$ nature). Importantly, as can be seen in the Supporting Information, the n-orbital associated with the $1^1n-\pi^*$ nature of the S₁ states involves the carbamoyl substituent of nicotinamide and NBzOx (rather than the nitrogen heteroatom). Finally, a 0.37 eV energy barrier separates the minimum of S₁ with an MECI that involves the ground state. Along the MEP, the main geometrical distortions involve a torsion of the NH₂ group, while the ring remains relatively flat. Thus, the accessibility of the MEP to the crossings between S₃/S₂ and later the S₂/S₁ surfaces, as well as the change in nature from $1^1\pi-\pi^*$ to $1^1n-\pi^*$ states, is fully consistent with the subpicosecond decay of the originally excited bright state observed in the upconversion experiments, as well as the subsequent formation and decay of emissive dark states shown in the transient absorption results. While two $1^1n-\pi^*$ states exist below S₃, the population of the upper $1^1n-\pi^*$ S₂ state is likely to correspond to a kinetic steady-state situation. That is, the population does not accumulate in this state but rather serves as a gateway into the lowest-energy $n-\pi^*$ state.

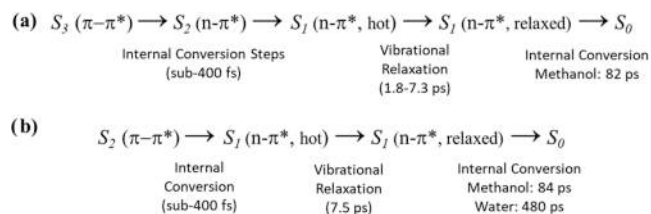
Similar conclusions to those of CMP arise from the analysis of the MEP for nicotinamide, as shown in Figure 9c. For this molecule, proceeding from the bright $\pi-\pi^*$ S₂ state, the system evolves directly to a deep minimum of the S₁ state of a dark $1^1n-\pi^*$ nature. In this case, the calculations show a significant energy barrier of 0.81 eV to access an MECI with the ground state from the S₁ state. In both oxidized-type molecules, the structural changes on the carbamoyl moiety are practically the same on the final part of the MEP.

The drastic differences in the experimental observations between the reduced and oxidized forms of the nicotinamidic systems can be clearly explained on the basis of the computational results. In the reduced form, the first excited singlet has $\pi-\pi^*$ character and has a significant oscillator strength. Also, the calculations for CMDHP show the presence

of a significant energy barrier (0.14 eV) to reach a crossing region with the electronic ground state, which is consistent with a 510 ps lifetime of this emissive excited state. On the other hand, in the oxidized systems, there is a different ordering in the singlet manifold. Specifically, the bright π - π^* singlet associated with the first absorption bands shown in Figure 2 corresponds with a higher excited singlet (S_2 in nicotinamide and S_3 in NBzOx), and the first excited singlet has a nonemissive nature but can be detected by transient absorption experiments through their $S_1 \rightarrow S_n$ transitions.

Photophysical Pathways and Comparison with Other Heterocycles. Overall, the calculations are in full agreement with the experimental results, which show a long-lived emissive S_1 state for NBz. For NBzOx and nicotinamide, the data and the calculations are consistent with a subpicosecond decay of the original spectroscopic state and the presence of dark states with lifetimes of tens to hundreds of picoseconds. For the oxidized nicotinamidic molecules, the intermediate (few picoseconds) evolution of the transient absorption band centered at 425 nm is also consistent with a process of vibrational energy relaxation within the nonemissive S_1 state as indicated by the blue shift and narrowing of the $S_1 \rightarrow S_n$ transient band within the first 10 ps (see Figures 4c, 5c, and 6c). A summary of the photophysics of the oxidized forms of the nicotinamidic chromophores is included in Scheme 3.

Scheme 3. Photophysical Processes for the Reduced Nicotinamidic Chromophores: (a) NBzOx and (b) Nicotinamide



Next, we discuss our results in the context of previous studies of the pyridinic heterocycles, the parent chromophores of the oxidized nicotinamides. The two kinds of molecular systems have similarities, although they are structurally different due to the carbamoyl substitution in nicotinamide and its derivatives. The most elaborate study of the femtosecond and picosecond dynamics of pyridine was performed by Zhong et al.²⁴ in the gas phase, and Chachisvillis et al.²³ in the solution phase. The solution transient absorption studies for excitation into the S_2 ($^1\pi$ - π^*) state of pyridine observed the presence of a 2 ps decay component, followed by a slower, 23 ps component. The authors of this study also mentioned the presence of 100 to 200 fs components which were partially masked by solvent effects near $t = 0$. Importantly, besides the two decay components, the transient absorption traces of Chachisvillis et al. showed the clear presence of persistent transient absorption signals which did not show any decay at least in the time window of several nanoseconds for pyridine. The 23 ps component was assigned to the decay of the S_1 (n - π^*) state. This assignment implied that the 2 ps component is due to the evolution of the optically formed S_2 state, which decays through internal conversion to the lower excited singlet, possibly with geometric changes associated with a prefulvenic geometry. According to Chachisvillis et al., the 23 ps S_1 decay was assigned to channels that include both

intersystem crossing^{58,59} and relaxation to the electronic ground state including the possibility of crossing to other isomer conformers.²³ The presence of an intersystem crossing channel (similar to the present case for nicotinamide) was based on the presence of a long-lived species in the transient absorption signals, which were assigned as the lowest-energy triplet of pyridine, although a contribution to the signal by the prefulvenic isomer was also considered as a possibility.

A comparison between the dynamics of pyridine and those of nicotinamide and the quaternized nicotinamide molecule NBzOx shows both similarities and differences. First, in both cases, the fluorescence yield is minimal (of the order of 10^{-5}).²³ On the other hand, for NBzOx, the transient absorption signals decay to the baseline within our signal-to-noise ratio. This implies that the formation of triplet states upon excitation of NBzOx is at most a few percent, while for nicotinamide and pyridine, this channel is more significant. Also, the evolution of the bright state in NBzOx and nicotinamide toward the dark states is faster (~ 400 fs vs 2 ps) as evidenced by the present upconversion experiments. The main reason for the differences between the nicotinamidic chromophores and the pyridine heterocycle is most likely related to carbamoyl substitution. This group extends the electronic conjugation and is related to energy shifts within the singlet manifold and between the singlet and triplet manifolds, thus changing the couplings between the different potential energy surfaces associated with different multiplicity states or isomer forms.

Other important heterocycles have also been shown to have similar decay mechanisms after photoexcitation. Transient absorption studies of several pyrimidines, including different DNA and RNA components have shown that there are similar longer-lived (more than 10 ps) dark states which participate in a cascade-like electronic relaxation from the original bright $^1\pi$ - π^* states.^{12,42,43,54,55} For several of these pyrimidines, this $S_2 \rightarrow S_1 \rightarrow S_0$ sequence occurs in parallel with a direct ground-state repopulation channel ($S_2 \rightarrow S_0$) which can account for a fraction of the original excited population. For example, for 1-cyclohexyluracil, 60% of excited molecules evolves directly toward the ground state on a subpicosecond timescale, while the rest of the population evolves through a dark intermediary state.⁶⁰ Another example corresponds to nucleotides, nucleosides, and free pyrimidine bases including cytidine 5-monophosphate, 2-deoxycytidine (dCyd), and 2-deoxycytidine 5-monophosphate which form these types of intermediary dark n - π^* states with lifetimes from 10 to 150 ps.⁵⁵ In those studies, it was pointed out that the population of higher vibrational levels in the intermediary state from the first internal conversion step could be related to the rate of the second population transfer from the dark excited state to the electronic ground state.

Similar to the case of NAD⁺ and nicotinamide, the absence of steady-state fluorescence in the other systems is directly related to the presence of the cascade-like pathways, together with the nonradiative nature of the intermediary excited state. Much has been written in relation to the importance of these efficient mechanisms for the disposal of electronic excitation energy in the components of nucleic acids.^{12,61} For crucial biological chromophores, these kinds of photophysical channels are likely to contribute to an intrinsic photostability which was of particular relevance in prebiotic periods as well as in the initial evolutionary stages, when the earth surface was subject to intense UV irradiation.²¹ For the case of the

nicotinamide-type chromophores, this pathway is also related to an intrinsic photostability and sunscreen-type effects which have been mentioned in studies about the topical use of nicotinamide formulations for dermatological photoprotection.^{15,18}

CONCLUSIONS

We studied the primary photophysical channels of model systems for the understanding of the excited states of nicotinamidic chromophores. Both the reduced and oxidized forms of this chromophore had not been studied previously with femtosecond resolution nor at an appropriate computational level. We observed that upon excitation into the first or higher band of the reduced form of the model system NBz, a long-lived emissive excited state was observed with simple photophysics which only include solvation and relaxation processes within the first few picoseconds in the S_1 ($^1\pi-\pi^*$) state. The fluorescent excited state of this system has a lifetime of 510 ps.

The oxidized model systems show drastically different excited-state dynamics. Both model systems of our study, NBzOx and nicotinamide, show similar dynamics. The oxidized systems are heteroaromatic, while in NBz, the chromophoric unit corresponds to a linear conjugated system of two double bonds in the ring, extending through the heteroatom and involving the carbamoyl moiety. Also, differently from the reduced form, NBzOx and nicotinamide have a higher-lying bright state of $\pi-\pi^*$ nature (S_3 in NBzOx and S_2 for nicotinamide). Both the experimental and computational results show that upon excitation into this state, an ultrafast internal conversion takes place, populating lower excited dark singlet states of $n-\pi^*$ character, which was assigned as the second singlet excited state. The transient absorption signals associated with the S_1 state decay with a time constant of 80 ps (NBzOx) to 480 ps (nicotinamide in aqueous solution). The present results clarify the fundamental photophysical channels that dictate the drastically different excited-state processes for the reduced vs oxidized forms of the nicotinamidic chromophore.

ASSOCIATED CONTENT

Supporting Information

The Supporting Information is available free of charge at <https://pubs.acs.org/doi/10.1021/acs.jpcb.3c03246>.

Fluorescence upconversion results and fit parameters; solvent-only transient absorption scans; evolution of the bandwidth of the 425 nm transient absorption band of nicotinamide; and molecular equilibrium structures and energy calculations (PDF)

AUTHOR INFORMATION

Corresponding Author

Jorge Peon – Instituto de Química, Universidad Nacional Autónoma de México, Circuito Exterior, Ciudad Universitaria, Ciudad de México 04510, México; orcid.org/0000-0002-4571-5136; Email: jpeon@unam.mx

Authors

Mariana M. Reza – Instituto de Química, Universidad Nacional Autónoma de México, Circuito Exterior, Ciudad Universitaria, Ciudad de México 04510, México

Jesús Durán-Hernández – Instituto de Química, Universidad Nacional Autónoma de México, Circuito Exterior, Ciudad Universitaria, Ciudad de México 04510, México

Beatriz González-Cano – Instituto de Química, Universidad Nacional Autónoma de México, Circuito Exterior, Ciudad Universitaria, Ciudad de México 04510, México

Jesús Jara-Cortés – Unidad Académica de Ciencias Básicas e Ingenierías, Universidad Autónoma de Nayarit, Tepic 63155, México; orcid.org/0000-0002-2296-6119

Rafael López-Arteaga – Instituto de Química, Universidad Nacional Autónoma de México, Circuito Exterior, Ciudad Universitaria, Ciudad de México 04510, México; orcid.org/0000-0001-8058-3469

Andrea Cadena-Cacedo – Instituto de Química, Universidad Nacional Autónoma de México, Circuito Exterior, Ciudad Universitaria, Ciudad de México 04510, México

Leonardo Muñoz-Rugeles – Instituto de Química, Universidad Nacional Autónoma de México, Circuito Exterior, Ciudad Universitaria, Ciudad de México 04510, México

Jesús Hernández-Trujillo – Departamento de Física y Química Teórica, Facultad de Química, UNAM, Ciudad de México 04510, México; orcid.org/0000-0002-8657-9169

Complete contact information is available at:

<https://pubs.acs.org/doi/10.1021/acs.jpcb.3c03246>

Notes

The authors declare no competing financial interest.

ACKNOWLEDGMENTS

The authors acknowledge CONACYT-México grant Ciencia de Frontera 2019-51496 and PAPIIT/DGAPA/UNAM IG200621 for financial support and DGTIC-UNAM project LANCAD-UNAM-DGTIC-210 for computer time. J.J.-C. thanks Patronato-UAN grant Productividad Universitaria.

REFERENCES

- (1) Binder, D. K.; Scharfman, H. E. *Lehninger: Principles of Biochemistry*, 4th ed.; Nelson, D. L.; Cox, M. C.; Freeman, W. H., Eds.; Macmillan, 2004.
- (2) Yaseen, M. A.; Sutin, J.; Wu, W.; Fu, B.; Uhlir, H.; Devor, A.; Boas, D. A.; Sakadzic, S. Fluorescence Lifetime Microscopy of NADH Distinguishes Alterations in Cerebral Metabolism in Vivo. *Biomed. Opt. Express* **2017**, *8*, No. 2368.
- (3) Stringari, C.; Edwards, R. A.; Pate, K. T.; Waterman, M. L.; Donovan, P. J.; Gratton, E. Metabolic Trajectory of Cellular Differentiation in Small Intestine by Phasor Fluorescence Lifetime Microscopy of NADH. *Sci. Rep.* **2012**, *2*, No. 568.
- (4) Skala, M. C.; Ricking, K. M.; Bird, D. K.; Gendron-Fitzpatrick, A.; Eickhoff, J.; Eliceiri, K. W.; Keely, P. J.; Ramanujam, N. In Vivo Multiphoton Fluorescence Lifetime Imaging of Protein-Bound and Free Nicotinamide Adenine Dinucleotide in Normal and Precancerous Epithelia. *J. Biomed. Opt.* **2019**, *12*, No. 024014.
- (5) Lakowicz, J. R.; Szmajdzinski, H.; Nowaczyk, K.; Johnson, M. L. Fluorescence Lifetime Imaging of Free and Protein-Bound NADH. *Proc. Natl. Acad. Sci. U.S.A.* **1992**, *89*, 1271–1275.
- (6) Chance, B.; Cohen, P.; Jobsis, F.; Schoen, B. Intracellular Oxidation-Reduction States in Vivo. *Science* **1962**, *137* (1979), 499–508.
- (7) Galbán, J.; Sanz-Vicente, I.; Navarro, J.; de Marcos, S. The Intrinsic Fluorescence of FAD and Its Application in Analytical Chemistry: A Review. *Methods Appl. Fluoresc.* **2016**, *4*, No. 042005.
- (8) Cadena-Cacedo, A.; González-Cano, B.; López-Arteaga, R.; Esturau-Escofet, N.; Peon, J. Ultrafast Fluorescence Signals from β -Dihydropyridinone Adenine Dinucleotide: Resonant Energy Trans-

- fer in the Folded and Unfolded Forms. *J. Phys. Chem. B* **2020**, *124* (3), 519–530.
- (9) Cao, S.; Li, H.; Liu, Y.; Zhang, M.; Wang, M.; Zhou, Z.; Chen, J.; Zhang, S.; Xu, J.; Knutson, J. R. Femtosecond Fluorescence Spectra of NADH in Solution: Ultrafast Solvation Dynamics. *J. Phys. Chem. B* **2020**, *124* (5), 771–776.
- (10) Hull, R. V.; Conger, P. S., III; Hoobler, R. J. Conformation of NADH Studied by Fluorescence Excitation Transfer Spectroscopy. *Biophys. Chem.* **2001**, *90*, 9–16.
- (11) Michaelian, K.; Simeonov, A. Fundamental Molecules of Life Are Pigments Which Arose and Co-Evolved as a Response to the Thermodynamic Imperative of Dissipating the Prevailing Solar Spectrum. *Biogeosciences* **2015**, *12* (16), 4913–4937.
- (12) Middleton, C. T.; de La Harpe, K.; Su, C.; Law, Y. K.; Crespo-Hernández, C. E.; Kohler, B. DNA Excited-State Dynamics: From Single Bases to the Double Helix. *Annu. Rev. Phys. Chem.* **2009**, *60*, 217–239.
- (13) Gorbunova, I. A.; Sasin, M. E.; Golyshv, D. P.; Semenov, A. A.; Smolin, A. G.; Beltukov, Y. M.; Vasyutinskii, O. S. Two-Photon Excited Fluorescence Dynamics in Enzyme-Bound NADH: The Heterogeneity of Fluorescence Decay Times and Anisotropic Relaxation. *J. Phys. Chem. B* **2021**, *125* (34), 9692–9707.
- (14) Li, H.; Cao, S.; Chen, J.; Zhang, S.; Xu, J.; Knutson, J. R. Ultrafast Fluorescence Dynamics of NADH in Aprotic Solvents: Quasi-Static Self-Quenching Unmasked. *J. Photochem. Photobiol., A* **2023**, *436*, No. 114384.
- (15) Damian, D. L. Photoprotective Effects of Nicotinamide. *Photochem. Photobiol. Sci.* **2010**, *9* (4), 578–585.
- (16) Boo, Y. C. Mechanistic Basis and Clinical Evidence for the Applications of Nicotinamide (Niacinamide) to Control Skin Aging and Pigmentation. *Antioxidants* **2021**, *10* (8), No. 1315.
- (17) Snaidr, V. A.; Damian, D. L.; Halliday, G. M. Nicotinamide for Photoprotection and Skin Cancer Chemoprevention: A Review of Efficacy and Safety. *Exp. Dermatol.* **2019**, *28*, 15–22.
- (18) Gensler, H. L. Prevention of photoimmunosuppression and photocarcinogenesis by topical nicotinamide. *Nutr. Cancer* **2009**, *29* (2), 157–162.
- (19) Namazi, M. R. Nicotinamide in Dermatology: A Capsule Summary. *Int. J. Dermatol.* **2007**, *46* (12), 1229–1231.
- (20) Gustavsson, T.; Markovitsi, D. Fundamentals of the Intrinsic DNA Fluorescence. *Acc. Chem. Res.* **2021**, *54* (5), 1226–1235.
- (21) Beckstead, A. A.; Zhang, Y.; de Vries, M. S.; Kohler, B. Life in the Light: Nucleic Acid Photoproperties as a Legacy of Chemical Evolution. *Phys. Chem. Chem. Phys.* **2016**, *18* (35), 24228–24238.
- (22) Markovitsi, D.; Talbot, F.; Gustavsson, T.; Onidas, D.; Lazzarotto, E.; Marguet, S. Complexity of Excited-State Dynamics in DNA. *Nature* **2006**, *441* (7094), No. E7.
- (23) Chachisvilis, M.; Zewail, A. H. Femtosecond Dynamics of Pyridine in the Condensed Phase: Valence Isomerization by Conical Intersections. *J. Phys. Chem. A* **1999**, *103*, 7408–7418.
- (24) Zhong, D.; Diau, E. W. G.; Bernhardt, T. M.; De Feyter, S.; Roberts, J. D.; Zewail, A. H. Femtosecond Dynamics of Valence-Bond Isomers of Azines: Transition States and Conical Intersections. *Chem. Phys. Lett.* **1998**, *298*, 129–140.
- (25) Paul, C. E.; Gargiulo, S.; Opperman, D. J.; Lavandera, I.; Gotor-Fernández, V.; Gotor, V.; Taglieber, A.; Arends, I. W. C. E.; Hollmann, F. Mimicking Nature: Synthetic Nicotinamide Cofactors for C = C Bioreduction Using Enoate Reductases. *Org. Lett.* **2013**, *15*, 180–183.
- (26) López-Arteaga, R.; Peon, J. Ultrafast Photoluminescence Kinetics from Hot Excitonic States in CdSe Nanocrystals. *J. Phys. Chem. C* **2018**, *122*, 26698–26706.
- (27) Rodríguez-Romero, J.; Guarín, C. A.; Arroyo-Pieck, A.; Gutiérrez-Arzaluz, L.; López-Arteaga, R.; Cortés-Guzmán, F.; Navarro, P.; Peon, J. Fluorophore Release from a Polymethinic Photoremovable Protecting Group Through a Nonlinear Optical Process. *ChemPhotoChem* **2017**, *1*, 397–407.
- (28) Rodríguez-Córdoba, W.; Noria, R.; Guarín, C. A.; Peon, J. Ultrafast Photosensitization of Phthalocyanines through Their Axial Ligands. *J. Am. Chem. Soc.* **2011**, *133* (13), 4698–4701.
- (29) Muñoz-Rugeles, L.; Gallardo-Rosas, D.; Durán-Hernández, J.; López-Arteaga, R.; Toscano, R. A.; Esturau-Escofet, N.; López-Cortés, J. G.; Peón, J.; Ortega-Alfaro, M. C. Synthesis and Photodynamics of Stilbenyl-Azopyrroles: Two-Photon Controllable Photoswitching Systems. *ChemPhotoChem* **2020**, *4* (2), 144–154.
- (30) BAGEL, Brilliantly Advanced General Electronic-structure Library. <http://www.nubakery.org> under the GNU General Public License.
- (31) Boldridge, D. W.; Morton, T. H.; Scott, G. W. Formation Kinetics and Quantum Yield of Photon-Induced Electron Ejection from NADH in Aqueous Solution. *Chem. Phys. Lett.* **1984**, *108*, 461–465.
- (32) Van den Berg, P. A. W.; Widengren, J.; Hink, M. A.; Rigler, R.; Visser, A. J. W. G. Fluorescence Correlation Spectroscopy of Flavins and Flavoenzymes: Photochemical and Photophysical Aspects. *Spectrochim. Acta, Part A* **2001**, *57* (11), 2135–2144.
- (33) Kalyanasundaram, K.; Colassis, T.; Humphry-Baker, R.; Savarino, P.; Barni, E.; Pelizzetti, E.; Grätzel, M. Luminescence, Charge-Transfer Complexes, and Photoredox Processes Involving N-Alkylnicotinamide/Dihydronicotinamide Surfactants. *J. Am. Chem. Soc.* **1989**, *111*, 3300–3311.
- (34) Jiao, X.; Peterson, E. M.; Harris, J. M.; Blair, S. UV Fluorescence Lifetime Modification by Aluminum Nanoapertures. *ACS Photonics* **2014**, *1*, 1270–1277.
- (35) *Principles of Fluorescence Spectroscopy*, 3rd ed.; Lakowicz, J. R., Ed.; Springer: New York, 2006; p 251.
- (36) Horng, M. L.; Gardecki, J. A.; Papazyan, A.; Maroncelli, M. Subpicosecond Measurements of Polar Solvation Dynamics: Coumarin 153 Revisited. *J. Phys. Chem. A* **1995**, *99* (48), 17311–17337.
- (37) Pal, S. K.; Peon, J.; Bagchi, B.; Zewail, A. H. Biological Water: Femtosecond Dynamics of Macromolecular Hydration. *J. Phys. Chem. B* **2002**, *106*, 12376–12395.
- (38) Pal, S. K.; Peon, J.; Zewail, A. H. Biological Water at the Protein Surface: Dynamical Solvation Probed Directly with Femtosecond Resolution. *Proc. Natl. Acad. Sci. U.S.A.* **2002**, *99*, 1763–1768.
- (39) Tan, X.; Gustafson, T. L.; Lefumeux, C.; Burdzinski, G.; Buntinx, G.; Poizat, O. Solvation Dynamics Probed by Femtosecond Transient Absorption Spectroscopy: Vibrational Cooling and Conformational Relaxation in S1 Trans-4,4'-Diphenylstilbene. *J. Phys. Chem. A* **2002**, *106* (14), 3593–3598.
- (40) Iwaki, L. K.; Dlott, D. D. Three-Dimensional Spectroscopy of Vibrational Energy Relaxation in Liquid Methanol. *J. Phys. Chem. A* **2000**, *104* (40), 9101–9112.
- (41) Ghukasyan, V.; Heikal, A. A. *Natural Biomarkers for Cellular Metabolism: Biology, Techniques, and Applications*; CRC Press, 2014.
- (42) Ma, C.; Cheng, C. C. W.; Chan, C. T. L.; Chan, R. C. T.; Kwok, W. M. Remarkable Effects of Solvent and Substitution on the Photo-Dynamics of Cytosine: A Femtosecond Broadband Time-Resolved Fluorescence and Transient Absorption Study. *Phys. Chem. Chem. Phys.* **2015**, *17* (29), 19045–19057.
- (43) Kosma, K.; Schröter, C.; Samoylova, E.; Hertel, I. V.; Schultz, T. Excited-State Dynamics of Cytosine Tautomers. *J. Am. Chem. Soc.* **2009**, *131* (46), 16939–16943.
- (44) Madsen, D.; Thomsen, C. L.; Thogersen, J.; Keiding, S. R. Temperature Dependent Relaxation and Recombination Dynamics of the Hydrated Electron. *J. Chem. Phys.* **2000**, *113*, 1126–1134.
- (45) Kloepper, J. A.; Vilchiz, V. H.; Lenchekov, V. A.; Lenchenkov, V. A.; Germaine, A. C.; Germaine, A. C.; Brandforth, S. E. The Ejection Distribution of Solvated Electrons Generated by the One-Photon Photodetachment of Aqueous I⁻ and Two-Photon Ionization of the Solvent. *J. Chem. Phys.* **2000**, *113*, 6288–6307.
- (46) Shi, X.; Long, F. H.; Lu, H.; Eisenthal, K. B. Electron Solvation in Neat Alcohols. *J. Phys. Chem. A* **1995**, *99*, 6917–6922.

- (47) Scheidt, T.; Laenen, R. Ionization of Methanol: Monitoring the Trapping of Electrons on the fs Time Scale. *Chem. Phys. Lett.* **2003**, *371* (3–4), 445–450.
- (48) Braem, O.; Penfold, T. J.; Cannizzo, A.; Chergui, M. A Femtosecond Fluorescence Study of Vibrational Relaxation and Cooling Dynamics of UV Dyes. *Phys. Chem. Chem. Phys.* **2012**, *14* (10), 3513–3519.
- (49) Dietzek, B.; Kiefer, W.; Hermann, G.; Popp, J.; Schmitt, M. Solvent Effects on the Excited-State Processes of Protochlorophyllide: A Femtosecond Time-Resolved Absorption Study. *J. Phys. Chem. B* **2006**, *110* (9), 4399–4406.
- (50) Pigliucci, A.; Duvanel, G.; Daku, L. M. L.; Vauthey, E. Investigation of the Influence of Solute-Solvent Interactions on the Vibrational Energy Relaxation Dynamics of Large Molecules in Liquids. *J. Phys. Chem. A* **2007**, *111* (28), 6135–6145.
- (51) Pigliucci, A.; Vauthey, E. Vibrational Relaxation Dynamics of Polyatomic Molecules in Solution. *Chimia* **2003**, *57* (4), No. 200.
- (52) Rousslang, K.; Allen, L.; Ross, J. B. A. Phosphorescence Maxima and Triplet State Lifetimes of NAD⁺ and ϵ -NAD⁺ in Ternary Complexes with Horse Liver Alcohol Dehydrogenase. *Photochem. Photobiol.* **1989**, *49* (2), 137–143.
- (53) Ross, J. B. A.; Rousslang, K. W.; Motten, A. G.; Kwiram, A. L. Base Interactions in the Triplet States of NAD⁺ and NADH. *Biochemistry* **1979**, *18* (9), 1808–1813.
- (54) Boldissar, S.; de Vries, M. S. How Nature Covers Its Bases. *Phys. Chem. Chem. Phys.* **2018**, *20* (15), 9701–9716.
- (55) Hare, P. M.; Crespo-Hernández, C. E.; Kohler, B. Internal Conversion to the Electronic Ground State Occurs via Two Distinct Pathways for Pyrimidine Bases in Aqueous Solution. *Proc. Natl. Acad. Sci. U.S.A.* **2007**, *104* (2), 435–440.
- (56) Kutateladze, A. G. *Computational Methods in Photochemistry*; CRC Press, 2005.
- (57) Crespo-Hernández, C. E.; Martínez-Fernández, L.; Rauer, C.; Reichardt, C.; Mai, S.; Pollum, M.; Marquetand, P.; González, L.; Corral, I. Electronic and Structural Elements That Regulate the Excited-State Dynamics in Purine Nucleobase Derivatives. *J. Am. Chem. Soc.* **2015**, *137*, 4368–4381.
- (58) Selco, J. I.; Holt, P. L.; Weisman, R. B. Nonradiative Relaxation of Pyridine Vapor: Transient Absorption Studies of Triplet State Formation, Decay, Quenching, and Structure. *J. Chem. Phys.* **1983**, *79*, 3269–3278.
- (59) Knight, A. E. W.; Parmenter, C. S. Radiative and Nonradiative Processes in the First Excited Singlet State of Azabenzene Vapors. *Chem. Phys.* **1976**, *15*, 85–102.
- (60) Hare, P. M.; Crespo-Hernández, C. E.; Kohler, B. Solvent-Dependent Photophysics of 1-Cyclohexyluracil: Ultrafast Branching in the Initial Bright State Leads Nonradiatively to the Electronic Ground State and a Long-Lived $1n\pi^*$ State. *J. Phys. Chem. B* **2006**, *110* (37), 18641–18650.
- (61) Kleinermanns, K.; Nachtigallová, D.; de Vries, M. S. Excited State Dynamics of DNA Bases. *Int. Rev. Phys. Chem.* **2013**, *32* (2), 308–342.